Hottinger Brüel & Kjær, Inc.
6855 Commerce Blvd,
Canton, MI 48187

To: Michael Bernitsas, President
Vortex Power Solutions
2512 Carpenter Road,
Ann Arbor, MI 48108

From: Patrick Eyo, Jake Horcher, Mateo Sanchez, Jonah Shifrin; Testing Engineers.

Subject: Characterization and Modeling of Electromagnetic Energy Harvester

Date: October 2, 2020

Distr: Dr. Gabriellla Cerrato, Head of the Acoustic Research Center

METHODS

For this task, two experiments were conducted in order to build mathematical models to evaluate the Vortex Power Solutions transducer and recommend the mass and resistance combination to be used in order to maximize extracted electrical power normalized to the mechanical frequency range of 15 to 45 [Hz]. The power maximization conditions will then be compared to theoretical power maximization in order to validate the use of the theoretical equation.

Equipment

An Eminence MSE Audio W801 loudspeaker with a shunt resistor of 0.10±0 .01 [Ω] was used to conduct all experiments. In addition, A Labworks ET-126B Electrodynamic Transducer and ADXL335 Accelerometer were used for the second experiment. An Agilent 33120A Function Waveform Generator with voltage accuracy error of 0.001% and resolution error of ±0.1 [mV] along with a Parasound Z.amp power amplifier provided power to the systems for all of the trials. A Bourns PWR221T-30-R100F Current Shunt Resistor with accuracy error of 1% was used to measure current across the resistor in the provided loudspeaker. The LabView 2014 program *Loudspeaker Main* was used to collect data. Impedance magnitude, phase angle, loudspeaker voltage and current across the shunt resistor were collected at varying input wave frequencies. For experiment one and experiment two, a set of washers were weighed using the OHAUS Scout Pro SP602 Scale, with resolution error of 0.005 [g],

Experiment 1: Free Vibration and the Theoretical Model

Experiment 1 provided the necessary data to create a model for estimating total electrical impedance of the system using the speaker parameter values: mechanical compliance (C_m), mechanical mass (M_m), inductance (L_e), force factor (Bl), electrical resistance (R_e), and mechanical resistance (R_m).

Setup

A *W801* speaker with a load stand attached to the internal cone was set on a PVC plastic stand and connected to a *cDAQ-9178*, a *Keysight 33500B Series* waveform generator, a *Parasound Zamp 3 Zone* amplifier, and *PWR221T-30 Series* power resistor used as a shunt resistor to measure the current through the system. The waveform generator and power amplifier drove the speaker via alligator clip connections. An image of the experimental set up is shown in Figure 1 below.

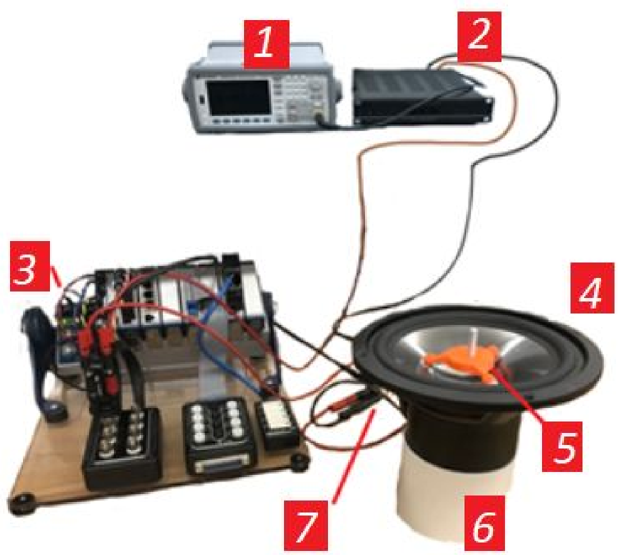

Legend
1. Waveform Generator
2. *Parasound Amp*
3. *cDAQ-9178*
4. *W801* Speaker
5. Load stand
6. PVC plastic stand
7. shunt resistor

Figure 1. This figure shows equipment used in the free vibration experiment. This image was captured before any masses or the securing nut were added.

Procedure

In order to empirically estimate these parameter values 10 trials were conducted: eight mass based trials consisting of coarse and fine sweeps centered around the resonant peak and two frequency sweeps on both the high end and low end of frequency (500-3500 [Hz] and 0.2-5 [Hz], respectively). Using four varied masses, zero through three mass washers, the LabView program cycled through a defined frequency range by a defined step size to create a Bode plot of electrical impedance for the system. First, a coarse sweep was completed to approximate the resonant frequency at each respective mass, followed by a fine sweep around the resonant peak with a smaller step size, in order to increase the resolution of each data set. The resonant frequency was identified as the first peak on the bode plot graphed by the program, with a step size of 1 [Hz]. This process was followed for each of the four masses. Additionally, high and low frequency sweeps were completed to provide further necessary data of the full frequency range. Three data points were taken at each frequency for all tests to allow for a calculation of precision error.

Model for Electrical Impedance

Measured electrical impedance of the speaker system (Z_e^{meas}) was calculated via the measurement of the current through the circuit ($I_{speaker}$) and the voltage drop across the speaker ($V_{speaker}$). The current through the circuit was calculated by using the resistance of the shunt resistor and the voltage drop across it as modeled in Equation 1 [1] below.

$$|Z_e^{meas}| = \frac{V_{speaker}}{I_{speaker}} \text{ where } I_{speaker} = \frac{V_{shunt}}{R_{shunt}} \quad \text{(Eqn. 1)}$$

The measured impedance is then decomposed into the resistance ($Re[Z_e^{meas}] = R_e^{meas}$) and reactance ($Im[Z_e^{meas}] = X_e^{meas}$) through Equations 2 [1] and Equation 3 [1].

$$Re[Z_e^{meas}] = R_e^{meas} = |Z_e^{meas}| cos(_e) \quad \text{(Eqn. 2)}$$

$$Im[Z_e^{meas}] = X_e^{meas} = |Z_e^{meas}| sin(_e) \quad \text{(Eqn. 3)}$$

In order to determine whether or not this data followed a mathematical model, a theoretical impedance was calculated in the same range of frequencies as recorded in the experiment. The theoretical model for electrical impedance Z_e^{tot} , given in Equation 4 [1], was derived by combining Lenz's law, Faraday's law, Kirchhoff's voltage and current law, and the equation of motion for the speaker cone/voice coil.

$$Z_e^{tot} = R_e + \frac{(Bl)^2 R_m}{R_m^2 + \left(\omega M_m - \frac{1}{\omega C_m}\right)^2} + j\left(\omega L_e - \frac{(Bl)^2 \left(\omega M_m - \frac{1}{\omega C_m}\right)^2}{R_m^2 + \left(\omega M_m - \frac{1}{\omega C_m}\right)^2}\right) \quad \text{(Eqn. 4)}$$

The model parameters are total mechanical resistance (R_m), total electrical resistance of the speaker (R_e), electrical inductance (L_e), total mechanical mass (M_m), total mechanical compliance (C_m), and force factor (Bl). These speaker parameters are determined from the measured impedance data acquired in the lab and are then used in Equation 4 to evaluate the validity of the model with respect to the experimental results for this class of transducers.

Parameter Calculation

Many parameters are calculated using slope values and intercept values of linear fits for different sections of the impedance data. For simplicity, in the equations shown below that describe how each parameter was calculated, slope and intercept values will be referenced using the standard form $y = m_n x + b_n$, where n references the figure number from which the slope or intercept was pulled.

Total Mechanical Compliance and Mechanical Mass

The total mechanical compliance and total mechanical mass of the speaker were calculated by finding the resonant frequency of the speaker at different mass loads utilizing the fine sweep data from the first test. The resonance frequency f_o , in Hz, and ω_o , in radians, are measured at the peak of the electrical impedance. This relation is demonstrated in Equation 5 [1]. Each added mass tested will yield a different resonance frequency.

$$\omega_o = 2\pi f_o = \sqrt{\frac{1}{C_m M_m}} \qquad \text{(Eqn. 5)}$$

Equation 6 [1] is an algebraic manipulation of Equation 5 where the slope, C_m, can be attained through graphing the relationship between ω_n^{-2} vs. the total system mass $(M_m + M')$.

$$\omega_n^{-2} = C_m (M_m + M') \qquad \text{(Eqn. 6)}$$

As shown by Equation 6, C_m is equal to the slope of the line of best fit calculated this way, m_3. M_m was calculated using the intercept of this line of best fit, b_3, and the algebraic manipulation of Equation 7 [1] below.

$$M_m = \frac{b_3}{Cm} \qquad \text{(Eqn. 7)}$$

Electrical Inductance and Force Factor

Electrical inductance, *Le*, is a parameter that can be determined by graphing the frequency f versus measured reactance, X_e^{meas}. At high frequencies, the slope, $m_{4,\,\mathrm{High}}$, of the line of best fit of this graph is a function of *Le,* shown in Equation 8 [1] below.

$$Le = \frac{m_{4,\,High}}{2\pi} \qquad \text{(Eqn. 8)}$$

Similarly, graphing the same data at low frequencies can be used to determine the force factor, Bl^2, of the speaker. At low frequencies, the slope, $m_{4,\,\mathrm{Low}}$, is dominated by a function of Bl^2, *Le*, and *Cm*, shown in Equation 9 [1].

$$Bl^2 = \frac{(\frac{m_{4,\,Low}}{2\pi} - Le)}{Cm} \qquad \text{(Eqn. 9)}$$

Electrical Resistance and Mechanical Resistance

Electrical resistance of the speaker, R_e, can be approximated by the finding the low frequency asymptote of the graph of measured resistance, R_e^{meas}, vs. frequency, f. The peak magnitude of the real portion of the impedance can then be used to approximate the value of mechanical resistance, R_m. This is because the magnitude of the imaginary portion, X_e^{meas}, of impedance approaches zero at this point. The fine sweep data from Experiment 1 was used to calculate the total mechanical resistance of the speaker. The peak measured resistance $R_e^{meas,\ max}$ is described by Equation 10 [1] which can be determined by the graphing f versus R_e^{meas}.

$$R_e^{meas,\ max} = R_e + \frac{(Bl)^2}{R_m} \qquad \text{(Eqn. 10)}$$

A manipulation of Equation 10 can be made to solve for R_m as seen in Equation 11 [1] below.

$$R_m = \frac{(Bl)^2}{R_e^{meas,\ max} - R_e} \qquad \text{(Eqn. 11)}$$

Experiment 2: Dynamic Motion Setup

In order to determine a mass-resistor combination that provides a maximum normalized power generation, a dynamic motion experiment was conducted. This experiment used a vibration exciter to introduce base motion similar to the vortex induced motion proposed by the Vortex Power Solutions design. These vibrations were produced by the input signal from the function generator and amplifier, in order to excite the speaker. A *LabView* program was used to take datum readouts from the accelerometer and speaker.

Setup

A few changes were made to the static examination setup for the dynamic motion trials. The *W801* Speaker was placed onto a *Bruel & Kjaer 4809* vibration exciter with rubber padding included under the exciter. On the metal frame of the speaker, an *ADXL355* accelerometer, accuracy error of ten percent, was attached. The speaker was also connected to the provided resistor bank by banana plug connections. The same waveform generator, power amplifier and cDAQ used in the static experiment were used in the dynamic experiment. An image of the added experimental equipment is shown in Figure 2 on the next page.

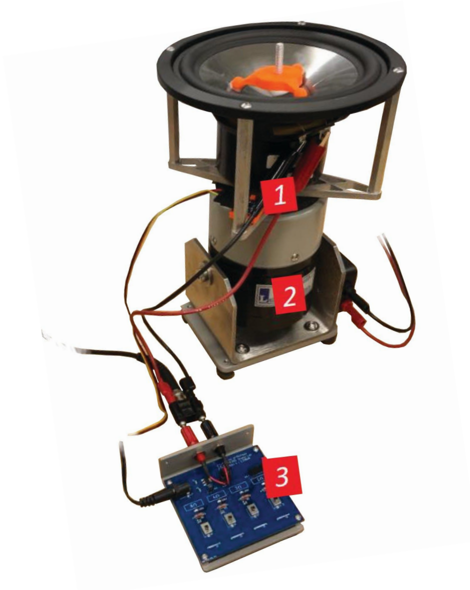

Legend
1. Accelerometer
2. *Vibration Exciter*
3. *Resistor Bank*

Figure 2. The image to the left articulates the key features of the dynamic motion setup.

Procedure

In order to create a Bode plot of the speaker impedance, a *LabView* program cycled through a defined frequency range. First, a coarse sweep was performed to identify the frequency range of the resonant peak, then a fine sweep was completed around the resonant peak with a smaller step size. We remained consistent with a fine sweep of ± 8 [Hz] of what we identified as the resonant frequency, with a step size of 1 [Hz]. This process was followed for each odd numbered resistor combination from 1 to 15 [Ω] and for each set of lumped masses, which was composed of three washers for the first set and five washers for the second.

Power Generated

To determine the power generated by the transducer, voltage was measured across the load resistance and was normalized by the acceleration measured by the accelerometer which is described in Equation 12 [1] below.

$$Normalized\ Power\ Output = \frac{V_L^{\ 2}}{2R_L|Accel|^2} \qquad \text{(Eqn. 12)}$$

The power generated was measured as a function of frequency and with three different mass values and eight different resistance values. This was done to determine the optimal combination of resistance and mass to maximize normalized power output, as well as to show how power output is dependent on frequency. The equation below shows the theoretical normalized power output [1].

$$Theoretical\ Normalized\ Power = \frac{R_L}{2} * \frac{(M_m\,Bl)^2}{Zm^2((R_L + Re[Z_e^{tot}])^{\,2} + Im[Z_e^{tot}]^2)} \qquad \text{(Eqn. 13)}$$

RESULTS

The data acquired for both static and dynamic tests were examined using *MATLAB* to configure important parameters needed to mathematically model the impedance of the system, as well as their respective errors. After all parameters were calculated, they were used in the theoretical mathematical model and this model was compared to experimental data to establish the validity of the model. Finally, different added masses and load resistance combinations were plotted against the normalized time-averaged power generated for these three masses and eight resistances and determining the optimal combination that yields the highest power output within the prescribed 15-45 [Hz] range.

Mathematical Modeling and Parameter Determination

The equations above were used to calculate the different parameters that are used in the theoretical model of the total impedance. These calculations are shown below.

Calculation of C_m and M_m

In order to calculate the unknown parameters in the mathematical model in Equation 4, three figures were generated. Figure 3 below was used to calculate the parameters C_m and M_m as described in the procedure where ω_n is representative of resonant frequency.

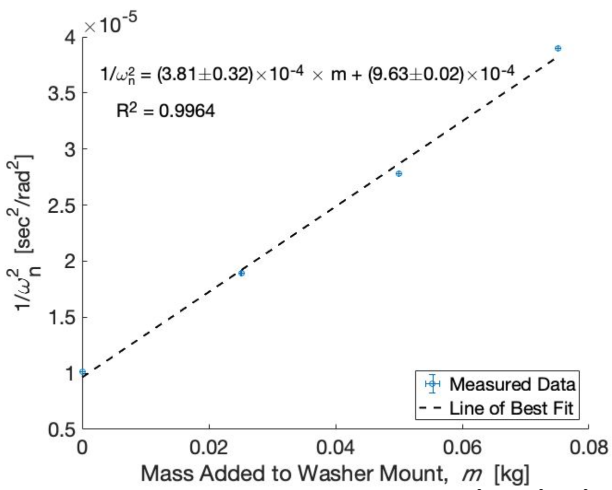

Figure 3. This figure plots added mass (kg) vs 1/(resonant frequency)^2 [sec^2/rad^2] in order to generate a line of best fit. The slope of this line articulates the equation parameter C_m. C_m was calculated to be (3.81±0.32)x10^{-4} [s^2/(kg*rad^2)]. The error bars articulate a maximum mass error of 2.29x10^{-5} [Hz] and a maximum vertical error of 1.53x10^{-10} [s^2/rad^2]. The intercept of the line of best fit is (9.63±0.02)x10^{-4} [s^2/rad^2].

Using the slope of this line of best fit for C_m, (3.81±0.32)x10^{-4} [s^2/(kg*rad^2)], M_m was calculated using the intercept of this line of best fit and Equation 7. The resulting M_m value is 0.025±0.0045 [kg].

Calculation of *Le* and *Bl*^{2}

Next, the high and low frequency test data was used to generate two frequency vs measured reactance graphs. Figure 4, below, shows these two plots which were used to calculate values for the parameters *Le* and *Bl*^{2} respectively.

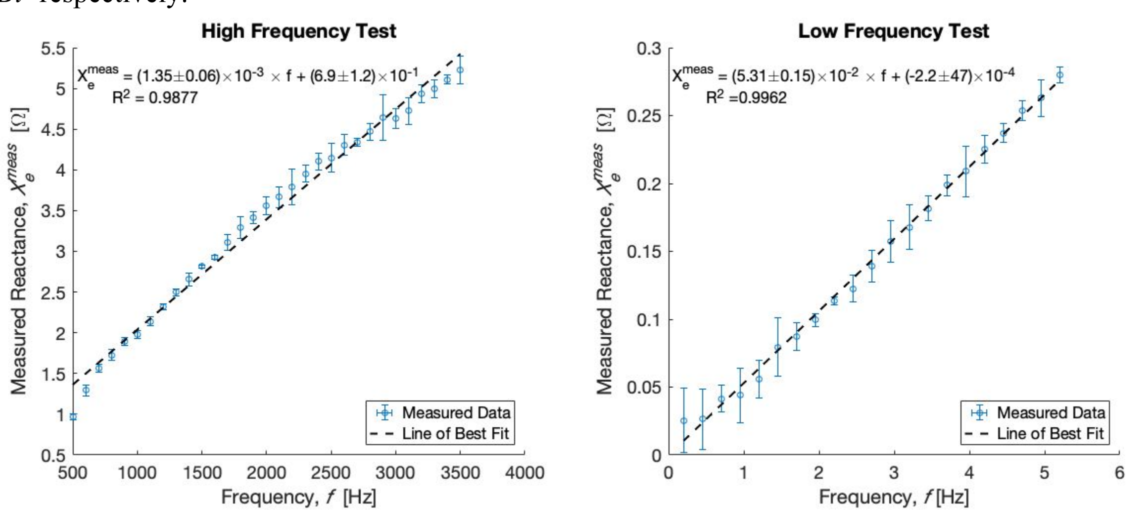

Figure 4. The left hand graph depicts the measured reactance [**Ω**] vs. a high frequency input signal. The right hand graph depicts the measured reactance vs. a low frequency signal input. Each graph shows a set of recorded data points with respective error bars as well as a line of best fit whose equation is listed in the plot. All of the following values are listed in the order of high then low frequency, respectively. The line of best fit slopes are (1.35±0.06)x10^{-3} [**Ω**-s] and (5.31±0.15)x10^{-2} [**Ω**-s]. The intercepts of each line of best fit are (6.9±1.2)x10^{-1} [**Ω**] and (-2.2±47)x10^{-4} [**Ω**]. The maximum frequency errors are 3.10x10^{-4} [Hz] and 2.36x10^{-4} [Hz]. The maximum measured reactance errors are 0.22 [**Ω**] and 0.02 [**Ω**].

At high frequencies, the slope of the graph is dominated by the 2π times the parameter *Le*, when plotted against frequency, as shown in Equation 8. Using the line of best fit slope value and Equation 8, *Le* was calculated to be (2.15±0.09)x10^{-4} [H]. Using Equation 9, Bl^2 was calculated to be 21.6±1.9 [(Tesla meters)^2].

Calculation of Re and Rm

In order to generate values for the electrical resistance, R_e, and mechanical resistance, R_m, the measured resistance vs. frequency was plotted. The low frequency asymptotic value of the real portion of impedance, with error, was used to determine the value of R_e. Figure 5 below displays this process.

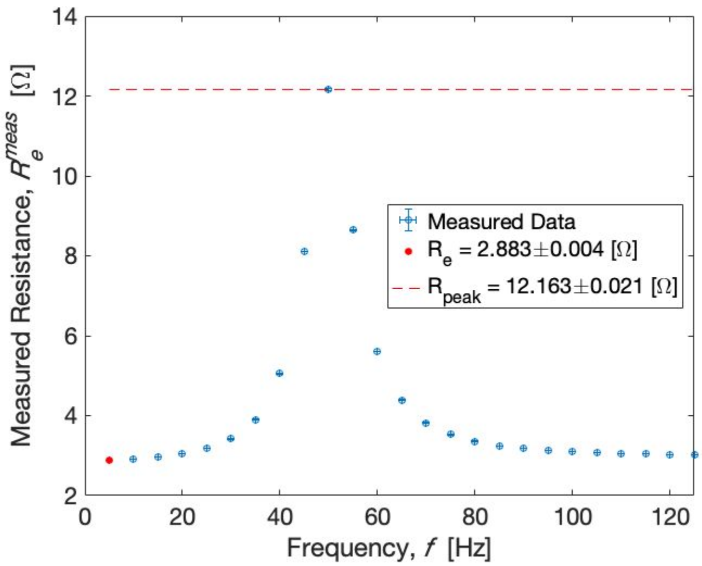

Figure 5. This figure depicts the real component of the measured impedance. The blue markers represent each recorded data point and its respective error. The maximum frequency error in this plot is 2.31x10^{-4} [Hz] and the maximum impedance error is 2.13x10^{-2} [**Ω**]. As seen above, the value for R_e is estimated as the first data point of the measured resistance, with a value of 2.88±4.4x10^{-3} [**Ω**]. The dashed red line indicates the peak of the resistance denoted as R_{peak}=12.16±2.10x10^{-2} [**Ω**].

The R_e value of 2.88±4.35x10^{-3} [**Ω**] was then used to calculate R_m using the value of the peak of the real portion of the impedance graph, R_{peak}, the parameter $(Bl)^2$, and Equation 11, where R_{peak} is equal to $R_e^{meas,\,max}$. Using this equation, the value of R_m was calculated to be 2.33±0.20 [**Ω**].

Impedance Model Validation

Having calculated all the previously unknown speaker parameters, a model for calculating theoretical impedance can be made by plugging these parameters into Equation 4. Table 1 below summarizes the values of the speaker parameters and their associated errors.

Table 1. Speaker parameters, and their associated errors, for use in the mathematical model of theoretical impedance.

Parameter	Value
Mechanical Compliance (C_m)	(3.81±0.32)x10^{-4} [s^2/(kg*rad^2)]
Mechanical Mass (M_m)	0.0253±0.0045 [kg]
Inductance (L_e)	(2.154±0.089)x10^{-4} [H]
Force factor $(Bl)^2$	21.6±1.9 [(Tesla meters)^2]
Electrical Resistance (R_e)	2.88±4.4x10^{-3} [**Ω**]
Mechanical Resistance (R_m)	2.33±0.20 [Ns/m]

By plugging the speaker parameters in Table 1 into Equation 4, the mathematical model for the impedance of the transducer was generated, and compared to the experimental data recorded in Experiment 2. The theoretical trendline and experimental data are plotted together in Figure 6 below for visual comparison.

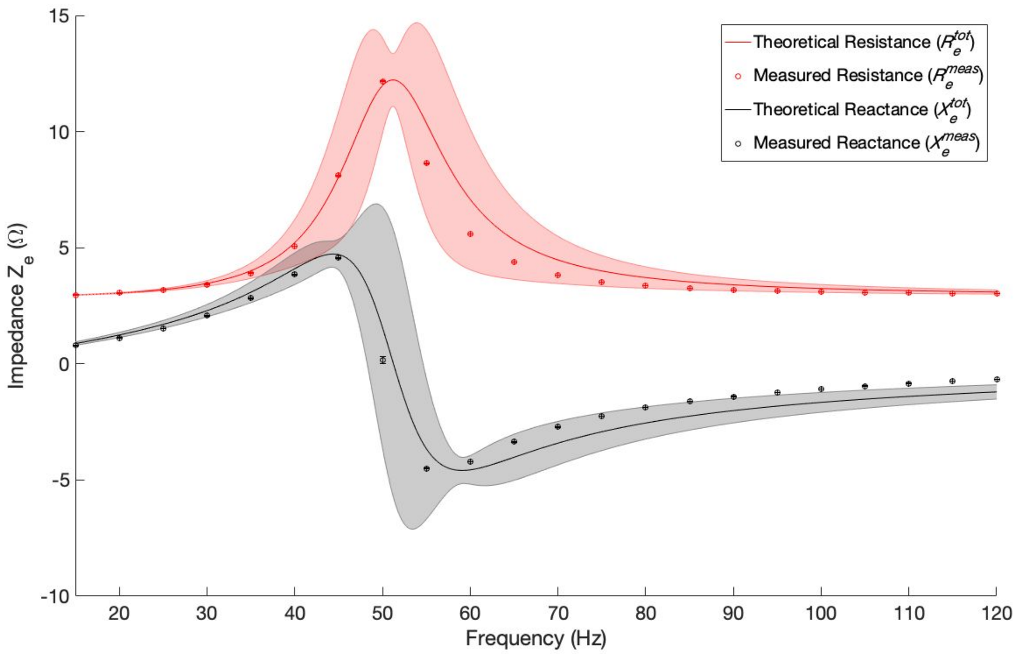

Figure 6. Theoretical impedance as compared to the experimental data. The shaded region indicates uncertainty in the mathematical model due to uncertainty in the calculated speaker parameters while error bars indicate uncertainty in measured values. Maximum uncertainty was ±4.1 [**Ω**] for theoretical resistance, R_e^{tot}; ±5.8 [**Ω**] for theoretical reactance, X_e^{tot}; ±0.021 [**Ω**] for measured resistance, R_e^{meas}; ±0.14 [**Ω**] for measured reactance, X_e^{meas}; and ±1.2 x 10^{-4} [Hz] for frequency. There are large uncertainties in the model at points of rapid change due to the calculation of uncertainty involving partial derivatives of the function in question.

As is shown by Figure 6, the theoretical model is a good fit for the system, as the measured data points almost all fit within the theoretical uncertainty of the model. The deviation of the measured data from the model may be due to losses within the equipment (wires, machines, etc.) or signal noise, since the magnitude of the recorded values are almost always lower in magnitude than the model predicts. This validates the model as a relatively accurate representation of this class of transducers for use in the ultimate design.

Maximizing Power

In order to inform a recommendation of what resistance mass and forcing frequency maximizes power generation, the eight different resistance trials were conducted each with a respective mass set of zero, three, and five washers. In each trial, load voltage and acceleration was recorded in order to plot a normalized power vs. load resistance graph and a normalized power vs. forcing frequency graph. First, the three normalized power vs. load resistance graphs were analyzed to determine the optimal resistance and mass for maximized power generation; the three graphs are depicted in Figure 7 below.

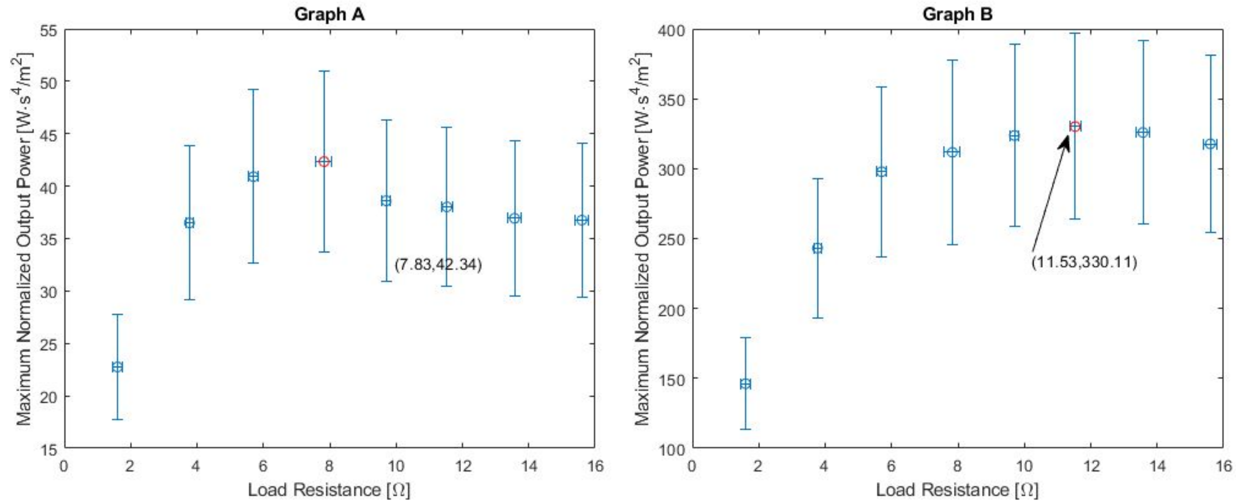

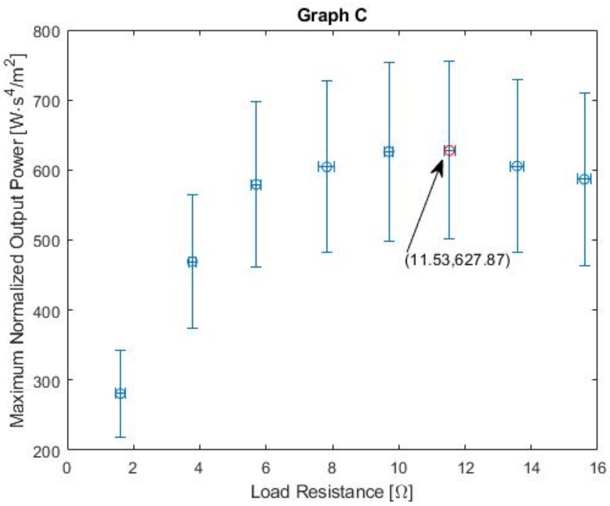

Figure 7. This figure depicts the relationship between the maximum normalized output power versus load resistance for the three respective mass sets. Graph A (top left) shows a maximum normalized power of 42.34±8.6 [W-s^4/m^2] at a load resistance of 7.83±0.24 [**Ω**] at zero added mass. Graph B (top right) shows a maximum normalized power of 330±67 [W-s^4/m^2] at a load resistance of 11.53±0.17 [**Ω**] at 75.39±0.021[g] of added mass. Graph C (bottom left) shows a maximum normalized power of 628±130 [W-s^4/m^2] at a load resistance of 11.53±0.17 [**Ω**] at 125.50±0.02 [g] of added mass. The large error bars from the graph can be attributed to the 10% accuracy error of the accelerometer.

With a maximum normalized power output of 628±130 [W-s^4/m^2], at a load resistance of 11.53±0.17 [**Ω**], the resistance and mass combination that is able to maximize power output is 11.53±0.17 [**Ω**] and 125.50±0.02 [g]. With this information, a normalized power output versus frequency graph was generated by sweeping through the frequency range of interest, 15-45 Hz, using the optimal mass-resistor combination. In order to better report the optimal forcing frequency we conducted a fine sweep over a 16-24 Hz range with a step size of 1 Hz. The resulting normalized power to forcing frequency relationship is depicted in Figure 8.

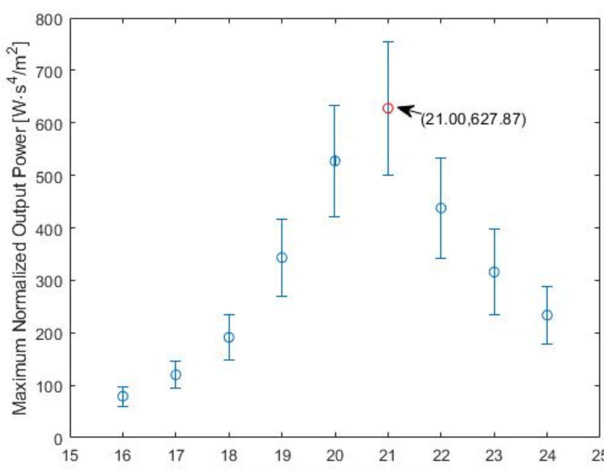

Figure 8. This image depicts the peak of the normalized power output of the experiment 2 setup vs. the forcing frequency within the prescribed 15-45 Hz range with the normalized power optimal mass and load resistance. The point in red depicts the experimental maximum normalized power output of 627.9±126.8 [W-s^4/m^2] at a forcing frequency of 21.00±5.0x10^{-4} [Hz]. The large error bars from the graph can be attributed to the 10% accuracy error of the accelerometer.

Recommendations

Based on the collected empirical data, the equipment, and specification defined in the work request, we recommend the use of 11.83±0.17 [**Ω**] load resistance and a 125.50±0.02 [g] added mass in order to maximize the power output of the proposed power generation system. If further tests were to be conducted, it is recommended to investigate the use of even larger added mass as the trends in our data indicate there may be further room to increase maximum power output of this system within the defined 15-45 Hz forcing frequency range. This hypothesis is supported by the trend within graphs A, B, and C of Figure 7 showing a direct relationship between added mass and maximum normalized power output. This is further corroborated by the theoretical equation for normalized time average power, Equation 13, which includes M_m in the numerator. This would suggest that adding mass would increase the maximum normalized time average power, however, other parameters in the denominator are functions of M_m, so the relationship between M_m and normalized time average power may not be exactly linear.

REFERENCES

[1] Beranek, LL (1986), *Acoustics*, AIP Press

[2] Dal Bo, L. and Gardonio P., 2019, "Energy harvesting with electromagnetic and piezoelectric seismic transducers:Unified theory and experimental validation." *Journal of Sound and Vibration 433*, pp. 385-424.

[3] Harbor Freight (n.d.).Voltmeter manual. Retrieved October 18, 2020, from https://manuals.harborfreight.com/manuals/98000-98999/98674.pdf

[4] National Instruments (2015). Datasheet NI 9225. Retrieved October 19, 2020, from http://www.ni.com/pdf/manuals/374184c_02.pdf

[5] Taylor, J.R. (1997), *An Introduction to Error Analysis*, 2nd ed., University Science Books, Sausalito, California.

[6] William J. Palm III (2013), *System Dynamics*, 3rd ed., McGraw-Hill, New York, NY